Zhanan Zou

Tiefeng Li[1]
e-mail: litiefeng@zju.edu.cn

Shaoxing Qu[1]
e-mail: squ@zju.edu.cn

Department of Engineering Mechanics,
Zhejiang University,
Hangzhou 310027, China;
Soft Matter Research Center (SMRC),
Zhejiang University,
Hangzhou 310027, China

Honghui Yu
Department of Mechanical Engineering,
City College of New York, CUNY,
New York, NY 10031

Active Shape Control and Phase Coexistence of Dielectric Elastomer Membrane With Patterned Electrodes

Various applications of dielectric elastomers (DEs) have been realized in recent years due to their lightweight, low cost, large actuation and fast response. In this paper, experiments and simulations are performed on the active shape control of DE structures with various two-dimensional patterned electrodes by applying voltage. A DE membrane with a pattern of electrodes is mounted on an air chamber. It is first inflated by air pressure and then further deformed by applying voltage, which actively controls the membrane shape. Under higher voltage, an acrylic membrane with larger actuation can induce shape instability and demonstrate multiphase coexistence behavior. In the framework of electromechanical theory, finite element simulations are carried out and the results are in good agreement with those obtained by experiments. [DOI: 10.1115/1.4025416]

1 Introduction

Dielectric elastomer (DE) membrane reduces thickness and expands area when subjected to an electric field through its thickness direction [1–5]. As a typical electroactive polymer (EAP), DE has a large actuation strain (over 300%), is light weight, has a fast response, and is low cost. It has various applications including adaptive optics, braille displays, microfluid control, and energy harvesting [6–13]. Suitably designed DE actuators using acrylic elastomers can be operated with giant voltage-induced deformation. Recent studies have shown voltage-induced expansion in area by 158% when a membrane is biaxially stretched and fixed to a rigid frame [7], and by up to 1689% when it is mounted in a chamber of compressed air [14]. In practical applications, "soft" robots require flexible components such as actuators and grippers, which provide multiple degrees of freedom to conform to their surroundings. Previous studies have shown that active materials such as shape memory alloy, hydrogel, and liquid crystal can be specifically arranged and combined with passive frames to build deformable structures [15]. Artificial muscles and smart structures based on DEs are widely attractive in the robotics field, which is attributed to their self-sensing and self-priming abilities [16].

While a DE membrane can produce large in-plane deformation by applying voltage, achieving three-dimensional shape control and out-of-plane deformation is challenging. The conventional design of active DE structure relies on combining passive skeleton frame and prestretched elastomer membrane, which results in complex 3D structures [17–20]. Complex motions and desired 3D shapes are difficult to obtain using the soft active zones in the passive frame and active membrane structures. To overcome the above difficulty, we adopt a different approach using 2D patterned electrodes to achieve active 3D shape control. First, a commercially available acrylic elastomer (3M-VHB 4905), coated with patterned electrodes, is inflated into a 3D configuration by air pressure. Then, various voltages are applied through the active zones (electrode-coated zones) to actively control the shape of the inflated membrane. With specific patterns of electrodes, large voltage-induced actuation and multiphase coexistence behavior are achieved. To predict the actuation behavior and to design the patterns of electrodes, a numerical method is developed for the deformation of DE membranes.

2 Experiments

Following the previous studies on DE membrane inflation [14,21–23], the experimental setup shown in Fig. 1 includes a DE membrane inflation actuator, a high voltage power source (Trek 610E), an air pump, a syringe, and an air pressure gauge. As shown in Fig. 2, the DE membrane inflation actuator is composed of a membrane module mounted on the air chamber. The circular DE membrane (3M-VHB 4905) has a diameter of 65 mm and is coated with two-dimensional patterns of electrodes (carbon grease) at two sides using mask pattern printing method. Air is pumped into the chamber through an air pump and a syringe. A pressure gauge is connected to the air chamber for pressure measurements.

The membrane module is designed for easy assembling so that membranes with different patterns of electrodes can be easily replaced. In the membrane module, the DE membrane is clamped by two acrylic glass rings and connected to two tin foil strips. A silicone rubber ring is installed between the rings and the bottom mount for air sealing. The air pressure in the chamber is measured using a U-tube pressure gauge. Following the previous studies [14], the volume of air chamber $V_{chamber}$ is fixed as 300 ml to restrain the excessive voltage induced actuation and to avoid electric breakdown. The membrane is initially mounted on the air chamber without prestretch. Air is pumped into the air chamber through a valve, and the membrane is inflated into a balloon. Previous studies on DE membrane inflation actuator have shown that properly pressurizing the membrane into a state near the verge of the instability can trigger giant actuation after voltage is applied [14]. To enhance the actuation stroke and sensitivity of active shape control, a syringe is connected to the air chamber for fine adjustment of pressure. The syringe can inflate the membrane near the snap-through state, which is away from the failure. When the membrane is inflated into that proper state, valves are closed, and the amount of air enclosed by the air chamber and the balloon is fixed. Then various voltages are applied through the active zones of the DE membrane to further shift the balloon towards larger deformations, to various 3D configurations. During the voltage actuation, the air inside the balloon and chamber is taken as ideal

[1]Corresponding author.

Manuscript received August 12, 2013; final manuscript received September 4, 2013; accepted manuscript posted September 12, 2013; published online October 29, 2013. Editor: Yonggang Huang.

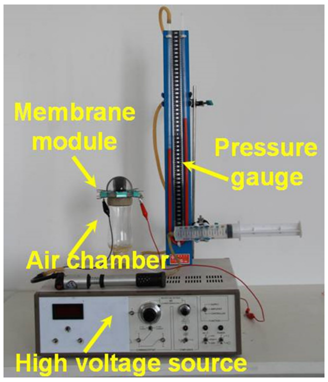

Fig. 1 A DE membrane (3M-VHB 4905) with patterned electrodes (carbon grease) is mounted on a chamber and inflated into a balloon. Voltages are applied through the active zones to further actuate the membrane.

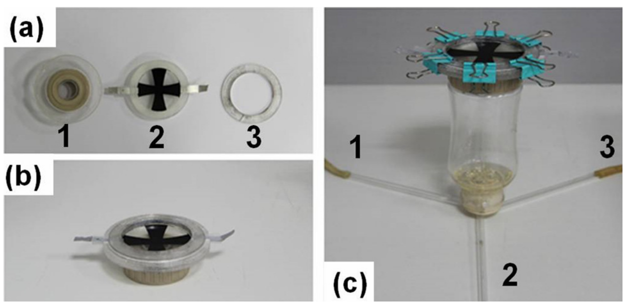

Fig. 2 (*a*) The membrane module (1—the bottom mount, 2—the membrane, and 3—the acrylic glass clip). (*b*) Assembling of the membrane module. (*c*) Membrane module is mounted on the air chamber. Three channels from air chamber are connected to the 1—pump, 2—syringe, and 3—pressure gauge.

gas. The pressure P in the balloon and chamber, and the volume of the balloon V_{balloon} are governed by

$$NkT = (V_{\text{chamber}} + V_{\text{balloon}}) \times (P_{\text{atm}} + P) \tag{1}$$

where N is the molecular number, kT represents the temperature in the unit of energy, and P_{atm} is the pressure of the surrounding atmosphere. We use video cameras to track the 3D shape of the balloon in both the top and side views simultaneously and record air pressure using the pressure gauge. In the experiments, inflation pressure is tuned around 20 mbar until the valves are closed. Voltages ranging from 0 to 7.5 kV are supplied by TREK 610E. As shown in Fig. 3, four different patterns of electrodes are chosen, tricircle (Fig. 3(*a*)), triangle (Fig. 3(*b*)), semicircle (Fig. 3(*c*)), and inner circle (Fig. 3(*d*)). Different 2D patterns of electrodes provide extensive range for active shape control. For instance, in the tricircle case (Fig. 3(*a*)), the patterned area can be actuated by voltage to form three antennas, and has the potential to be a soft gripper. In the inner-circle case (Fig. 3(*d*)), the curvature of the top area can be tuned fast and easily, and can be designed as soft lenses using transparent electrode techniques.

Furthermore, to enhance the voltage induced actuation, membranes with multiple layers are adopted. As shown in Fig. 4(*a*), two membranes (3M-VHB 4905) are stacked together. The top layer was cut through with three circular holes by laser cutter. Compliant electrodes are coated on both sides of the bottom layer only through the cut regions. This design provides the active zones larger preactuation deformation compared to the surrounding passive zones (Fig. 4(*b*)). By actuating these active zones, large voltage induced actuations are achieved (Fig. 4(*c*)).

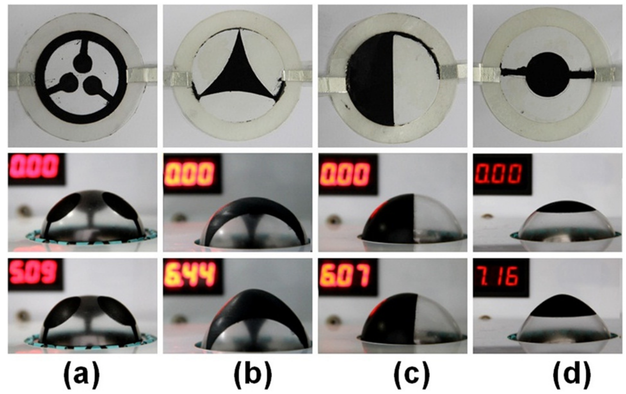

Fig. 3 The reference, pressurized, and actuated states of the membranes with different patterns of electrode (*a*)–(*d*). The first row shows the reference states, the second row shows the pressurized states, and the third row shows the voltage actuated states.

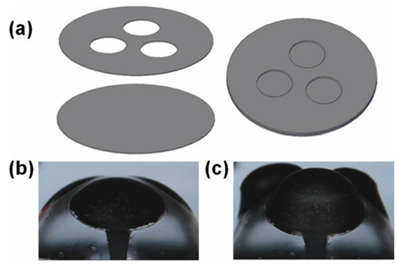

Fig. 4 (*a*) Schematics of two combined DE membranes structure. (*b*) Membranes in the state of preactuation. (*c*) Membranes in the actuated state by voltage.

3 Simulations

In order to guide the design of DE structures described in Sec. 2, we simulate the behaviors of DEs transducers using a finite element method based on the nonlinear field theory [24–26]. The method is implemented in the commercial finite element software ABAQUS, which provides a large library of functions to describe hyperelasticity. It can be used to solve electromechanical coupling problems of DE transducers with complex configurations and under inhomogeneous deformation. In the process of designing a new DE device, especially when the structure is complex, if a numerical simulation can predict how the performances and functionalities of the device depends on the material and geometric parameters, it would provide valuable guidance to the design and complements to traditional theoretical and experimental approaches.

The approaches developed by Zhao and Suo [27] and Qu and Suo [28] are applicable to solid elements but not membrane elements. When the balloon is inflated by air pressure, the membrane element is more suitable to describe the deformation than solid elements. In this study, we rewrite the equations of state in Zhao and Suo [27] and Qu and Suo [28] and develop a new USER-MATERIAL subroutine UMAT for membrane element to simulate the electromechanical coupling of DE structures. The Helmholtz free energy density function can be expressed as

$$W(\lambda_1, \lambda_2, D) = W_S(\lambda_1, \lambda_2) + \frac{D^2}{2\varepsilon} \tag{2}$$

in which the mechanical part and the electrical part are independent of each other. Following Qu and Suo's work [28], two sets of elements are adopted for the same set of nodes, but with different material properties, one for the mechanical model and the other

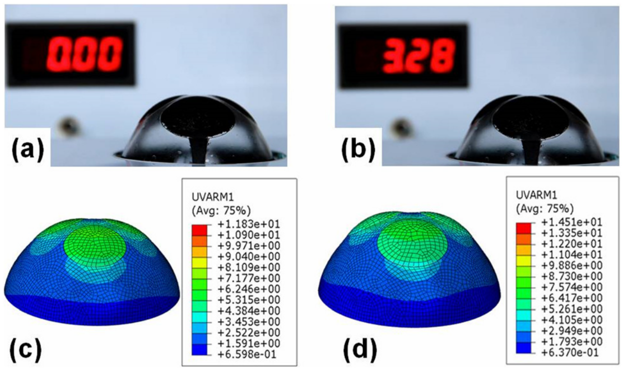

Fig. 5 The comparison between experimental and simulation results, (*a*) and (*c*) are the pressurized state without voltage, (*b*) and (*d*) are the actuated state by voltage

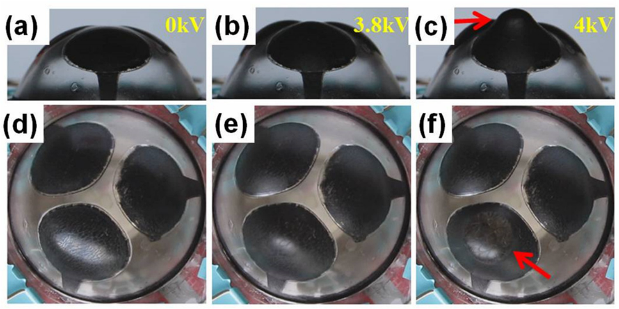

Fig. 6 The side and top views of inflated membranes, (*a*) and (*d*) three active zones of the DE membrane inflate out when only pressure is applied, (*b*) and (*e*) when voltage is applied, three active zones further inflate out, (*c*) and (*f*) when voltage reaches a certain level, a bulged zone and two unbulged zones coexist

for the electrical one. Since the stresses induced by mechanical deformation and electrical field are calculated at the Gaussian integration points of each set of elements separately, we developed a USER-VARIABLE subroutine (UVARM) to obtain the total stresses in ABAQUS.

We adopt the Neo-Hookean material model to simulate the actuation of the DE membrane. The DE membrane has the same two-layered design as in Sec. 2 to achieve large preactuation deformation and voltage actuation. Both sides of the DE membrane are coated with tricircle patterns of electrodes. Figures 5(*a*) and 5(*b*) show the preactuation state and the actuated state of the membrane by voltage. Figures 5(*c*) and 5(*d*) show the corresponding numerical results in three-dimensional Cartesian coordinate systems. UVARM1 denotes the stress along the x-direction, i.e., the horizontal direction of the membrane plane in the reference state. Numerical results are in good agreement with experimental ones. Huang recently developed a new constitutive framework for rubberlike materials with finite deformation [29], which can be used to predict the actuation behavior of DE membranes too.

4 Electromechanical Phase Coexistence

Figure 6 shows the two-phase coexistence behavior during actuation. When there is only pressure being applied, three active zones of the DE membrane inflate out with same deformation (Figs. 6(*a*) and 6(*d*)). Then a ramping up voltage is applied simultaneously to all three active zones. Under 3.8 kV voltage, all three active zones further inflate with same deformation (Figs. 6(*b*) and 6(*e*)).

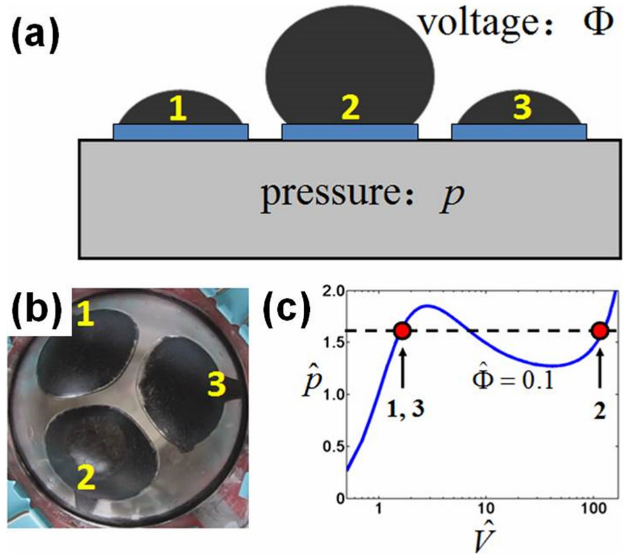

Fig. 7 (*a*) To simplify the calculation, the inflated tricircle membrane can be analyzed by three connected inflation membranes with the same voltage and pressure. One bulged section and two unbulged sections. (*b*) The coexisting bulged (zone 2) and unbulged (zones 1 and 3) states in the experiment. (*c*) The corresponding coexisting states on the calculated pressure-volume curve.

When the voltage reaches 4 kV, one active zone bulges out and coexists with the other two unbulged active zones (Figs. 6(*c*) and 6(*f*)). The "unbulge-to-bulge" phenomenon is analogous to the liquid-to-vapor phase transition. During actuation, the three active zones of the DE membrane form a composite thermodynamic system with the same voltage and pressure applied. Because the temperature is held constant, under the isothermal condition, the system reaches a state of equilibrium when the Helmholtz free energy of the system is stationary. The Helmholtz free energy of the composite is the sum of the Helmholtz free energy of each active zone. The condition of coexistence can be formulated following the previous approaches [25]. In the reference state, the bulged and the unbulged zones are of the same volume V. In the pressurized (pressure P) and the voltage actuated state (voltage Φ), the bulged and unbulged sections are in two different states of equilibrium. The bulged and unbulged zones are of different volumes V_1 and V_2 (the volume enclosed by the electrode-coated surface and the base plane formed by its edge), different charges Q_1 and Q_2, different electric displacements D_1 and D_2, and different deformation fields. To simplify the calculation, the inflated tricircle membrane is replaced by three connected inflation membranes with same voltage and pressure (Fig. 7(*a*)). Following the previous analysis of DE membrane inflation, in the absence of any applied load, the membrane is of a circular shape, thickness H, and radius A. The equations of state for the transducer can be expressed as follows:

$$\hat{p} = pA/\mu H = f(\hat{V}, \Phi/H\sqrt{\varepsilon/\mu}) \tag{3}$$

$$\hat{\Phi} = \Phi/H\sqrt{\varepsilon/\mu} = g(Q/A^2\sqrt{\varepsilon\mu}, \hat{p}) \tag{4}$$

where $\hat{V}$ is the dimensionless volume, defined as $\hat{V} = V/A^3$. We set the parameters as follows: shear modulus $\mu = 45\,\mathrm{kPa}$, permittivity $\varepsilon = 4.7\varepsilon_0$, where ε_0 is the permittivity of vacuum. These parameters are comparable with those reported in literature [14,30–32]. After calculation, the normalized pressure and volume curve is plotted in Fig. 7(*c*). The coexisting bulged (zone 2) and unbulged (zones 1 and 3) states, marked in Figs. 7(*a*) and 7(*b*), correspond to two states on the curve.

5 Conclusions

In summary, both the experiment and simulation show that the shape of a DE membrane with 2D patterned electrodes can be actively controlled by applying air pressure and voltage. Large voltage-induced actuation is demonstrated. The method for structural design and operation may be applicable in various applications of soft actuators. Furthermore, in a certain specific experimental setup, phase coexistence behavior is observed. Two stable states with significantly different actuation volume can coexist and be switched by voltage. This phase coexistence behavior may offer a novel way for actuation in soft robots and haptic feedback.

Acknowledgment

This work is supported by the National Natural Science Foundation of China (Nos. 11222218, 11302190, 11321202), Zhejiang Provincial Natural Science Foundation of China (Q13A020002), and the Fundamental Research Funds for the Central Universities (2013QNA4043).

References

[1] Hirai, T., Nemoto, H., Hirai, M., and Hayashi, S., 1994, "Electrostriction of Highly Swollen Polymer Gel: Possible Application for Gel Actuator," J. Appl. Polym. Sci., **53**(1), pp. 79–84.

[2] Liang, C., Sun, F., and Rogers, C., 1994, "Coupled Electro-Mechanical Analysis of Adaptive Material Systems—Determination of the Actuator Power Consumption and System Energy Transfer," J. Intell. Mater. Syst. Struct., **5**(1), pp. 12–20.

[3] Heydt, R., Kornbluh, R., Pelrine, R., and Mason, V., 1998, "Design and Performance of an Electrostrictive-Polymer-Film Acoustic Actuator," J. Sound Vib., **215**(2), pp. 297–311.

[4] Pelrine, R. E., Kornbluh, R. D., and Joseph, J. P., 1998, "Electrostriction of Polymer Dielectrics With Compliant Electrodes as a Means of Actuation," Sens. Actuators A, **64**(1), pp. 77–85.

[5] Zanna, J., Nguyen, H., Parneix, J., Ruffié, G., and Mauzac, M., 1999, "Dielectric Properties of Side Chain Liquid Crystalline Elastomers: Influence of Crosslinking on Side Chain Dynamics," Eur. Phys. J. B, **10**(2), pp. 345–351.

[6] Koh, S. J. A., Li, T., Zhou, J., Zhao, X., Hong, W., Zhu, J., and Suo, Z., 2011, "Mechanisms of Large Actuation Strain in Dielectric Elastomers," J. Polym. Sci. B, **49**(7), pp. 504–515.

[7] Pelrine, R., Kornbluh, R., Pei, Q., and Joseph, J., 2000, "High-Speed Electrically Actuated Elastomers With Strain Greater Than 100%," Science, **287**(5454), pp. 836–839.

[8] Carpi, F., De Rossi, D., and Kornbluh, R., 2008, *Dielectric Elastomers as Electromechanical Transducers: Fundamentals, Materials, Devices, Models and Applications of an Emerging Electroactive Polymer Technology*, Elsevier Science, Amsterdam.

[9] Anderson, I. A., Ieropoulos, I. A., Mckay, T., O'Brien, B., and Melhuish, C., 2011, "Power for Robotic Artificial Muscles," IEEE/ASME Trans. Mechatron., **16**(1), pp. 107–111.

[10] O'Brien, B. M., Calius, E. P., Inamura, T., Xie, S. Q., and Anderson, I. A., 2010, "Dielectric Elastomer Switches for Smart Artificial Muscles," Appl. Phys. A, **100**(2), pp. 385–389.

[11] Zhu, J., Kollosche, M., Lu, T., Kofod, G., and Suo, Z., 2012, "Two Types of Transitions to Wrinkles in Dielectric Elastomers," Soft Matter, **8**(34), pp. 8840–8846.

[12] Huang, J., Li, T., Chiang Foo, C., Zhu, J., Clarke, D. R., and Suo, Z., 2012, "Giant, Voltage-Actuated Deformation of a Dielectric Elastomer Under Dead Load," Appl. Phys. Lett., **100**(4), p. 041911.

[13] Wang, H., Cai, S., Carpi, F., and Suo, Z., 2012, "Computational Model of Hydrostatically Coupled Dielectric Elastomer Actuators," J. Appl. Mech., **79**, p. 031008.

[14] Li, T., Keplinger, C., Baumgartner, R., Bauer, S., Yang, W., and Suo, Z., 2012, "Giant Voltage-Induced Deformation in Dielectric Elastomers Near the Verge of Snap-Through Instability," J. Mech. Phys. Solids, **61**, pp. 611-628.

[15] Hawkes, E., An, B., Benbernou, N., Tanaka, H., Kim, S., Demaine, E., Rus, D., and Wood, R., 2010, "Programmable Matter by Folding," Proc. Natl. Acad. Sci., **107**(28), pp. 12441–12445.

[16] Mckay, T., O'Brien, B., Calius, E., and Anderson, I., 2010, "An Integrated, Self-Priming Dielectric Elastomer Generator," Appl. Phys. Lett., **97**(6), p. 062911.

[17] Kofod, G., Wirges, W., Paajanen, M., and Bauer, S., 2007, "Energy Minimization for Self-Organized Structure Formation and Actuation," Appl. Phys. Lett., **90**(8), p. 081916.

[18] Pei, Q., Rosenthal, M., Stanford, S., Prahlad, H., and Pelrine, R., 2004, "Multiple-Degrees-of-Freedom Electroelastomer Roll Actuators," Smart Mater. Struct., **13**(5), pp. N86–N92.

[19] Mckay, T., O'Brien, B., Calius, E., and Anderson, I., 2010, "Self-Priming Dielectric Elastomer Generators," Smart Mater. Struct., **19**(5), p. 055025.

[20] Kofod, G., Paajanen, M., and Bauer, S., 2006, "Self-Organized Minimum-Energy Structures for Dielectric Elastomer Actuators," Appl. Phys. A, **85**(2), pp. 141–143.

[21] Wissler, M., and Mazza, E., 2007, "Electromechanical Coupling in Dielectric Elastomer Actuators," Sens. Actuators A, **138**(2), pp. 384–393.

[22] Fox, J., and Goulbourne, N., 2009, "Electric Field-Induced Surface Transformations and Experimental Dynamic Characteristics of Dielectric Elastomer Membranes," J. Mech. Phys. Solids, **57**(8), pp. 1417–1435.

[23] Keplinger, C., Li, T., Baumgartner, R., Suo, Z., and Bauer, S., 2012, "Harnessing Snap-Through Instability in Soft Dielectrics to Achieve Giant Voltage-Triggered Deformation," Soft Matter, **8**(2), pp. 285–288.

[24] Suo, Z., 2010, "Theory of Dielectric Elastomers," Acta Mech. Solida Sinica, **23**(6), pp. 549–578.

[25] Lu, T.-Q., and Suo, Z.-G., 2012, "Large Conversion of Energy in Dielectric Elastomers by Electromechanical Phase Transition," Acta Mech. Sinica, **28**(4), pp. 1106–1114.

[26] Suo, Z., Zhao, X., and Greene, W. H., 2008, "A Nonlinear Field Theory of Deformable Dielectrics," J. Mech. Phys. Solids, **56**(2), pp. 467–486.

[27] Zhao, X., and Suo, Z., 2008, "Method to Analyze Programmable Deformation of Dielectric Elastomer Layers," Appl. Phys. Lett., **93**(25), p. 251902.

[28] Qu, S., and Suo, Z., 2012, "A Finite Element Method for Dielectric Elastomer Transducers," Acta Mech. Solida Sinica, **25**(5), pp. 459–466.

[29] Huang, Z.-P., 2013, "A Novel Constitutive Formulation for Rubberlike Materials in Thermoelasticity," ASME J. Appl. Mech. (accepted).

[30] Li, T., Qu, S., and Yang, W., 2012, "Electromechanical and Dynamic Analyses of Tunable Dielectric Elastomer Resonator," Int. J. Solids Struct., **49**, pp. 3754–3761.

[31] Li, T., Qu, S., and Yang, W., 2012, "Energy Harvesting of Dielectric Elastomer Generators Concerning Inhomogeneous Fields and Viscoelastic Deformation," J. Appl. Phys., **112**(3), p. 034119.

[32] Qu, S., Li, K., Li, T., Jiang, H., Wang, M., and Li, Z., 2012, "Rate Dependent Stress-Stretch Relation of Dielectric Elastomers Subjected to Pure Shear Like Loading and Electric Field," Acta Mech. Solida Sinica, **25**(5), pp. 542–549.